Optimized Multi-Objective Deep Learning with Enhanced Pair wise-Potential Activation Layer for Fiber Faults Identification

B. Vinothini[1], S. Sheeja[2]
[1]Department of CS, CA & IT
Karpagam Academy of Higher Education, Coimbatore, Tamil Nadu, India.
[2]Department of CS, CA & IT
Karpagam Academy of Higher Education, Coimbatore, Tamil Nadu, India.

ABSTRACT—
In textile commodities, the flaws recognition is the most time-consuming process which discovers the Fabric Defects (FDs) to boost the fabric quality. To combat this issue, an Enhanced Pair wise-Potential Activation Layer in Optimized Convolutional Neural Network (EPPAL-OCNN) model has been recently designed which solves the undesired convergence of CNN to increase the recognition rate. But, OCNN training needs more labeled samples and takes more time to label the fabric samples. Hence, this article designs an EPPAL- Optimized Multi-Criteria CNN (EPPAL-OMCCNN) model based on the multi-objective active sampling mechanism. The main aim of this model is to reduce the labeling time while considering more fabric samples for OCNN training. Initially, the OCNN structure is created using a limited amount of samples. After that, more influential samples are labeled based on the multi-objective sampling mechanism. By using these labeled samples, the OCNN is upgraded to recognize and categorize the FDs with the highest precision.Further, the test samples from the TILDA corpus are used to validate the EPPAL-OMCCNN which reveals that it attains 96.27% of accuracy compared to the classical models.

Keywords—Fiber defects recognition, EPPAL-OCNN, Image labelling, Active learning, Multi-objective sampling
DOI Number: 10.48047/NQ.2022.20.12.NQ773705 NeuroQuantology2022;20(12): 3814-3825

INTRODUCTION

Textile is a fundamental commodity that is commonly evolved. Microfiber threads are generally made from an organic substance. The maintenance stage demonstrates a weakness in the fabric's pattern. A faulty mounted tool or pattern shrinkage on the sewing process can cause substantial differences between the time of its development in filament, threads, or row

defects like leather misdrawing, materials, vagueness, and cotton damask [1]. Deficiencies can reduce operational costs by 45-65%. Weavers should regularly examine the fabric material for severe design flaws in modern spinners by navigating a couple of gadgets, as a material fault is prevented or remedied when recognized. As a result, the garment sector has advanced to fully computerized fiber examination for important fiber dependability calculations.

Artificial intelligence also termed learning is a grading technique that finds and highlights flaws in raw resources [2]. Cloth durability validation is generally the sole way to increase dependability, aiding in the timely and effective restoration of very minor flaws. Unfortunately, rigidity produces deformation, and minor flaws go unnoticed most of the

time. When compared to traditional findings, simple enhanced fabric screening improves the identification rate by roughly 80%. As a result, entirely computerized inspections are a viable option for enhancing apparel revenue when lowering operational costs [3]. Nonetheless, it can be difficult. Most modern fiber inspection models are vision-based, using image analyses and feature learning algorithms that frequently separate and detect degraded fabrics. The models for FD identification are classified as stochastic, empirical, structural, multimodal, learning, and template-based. These models appeared to be a failure, costly, involved with specific flaws and conflicting with differences in fiber productivity and form. Recently, a variety of models for identifying FDs were evolved [4].

Among several models, the upgraded version was designed to provide high longevity while dealing with variations in fiber patterns and defect grades. Conversely, it has proved less effective in detecting flaws than the recurrence unit of a structured fiber. Deep learner algorithms, such as CNN, were utilized to efficiently segregate fabric designs in the early modern era. CNN types [5-7] include Fully Convolutional Network (FCN), U-Net and others, that control essential blocks such as convolution, upsampling, and activation phases. But, it obtains characteristics alongside a whole context relationship and linguistics information which were useless for projecting appropriate visual qualities since standard CNNs are extensively scaled and confined variances were removed by pooling [8]. As a result, certain FDs were classified as restricted motifs since they were represented by minimal gray levels. An emergence of imperfections on fiber analogies, including overlapping, deterioration, granular groups, and so on, represents the major structural properties and frequently

comprises just about 35% of the pixels, leading to very imbalanced FD samples. To enhance restricted pattern localization, various practices were necessary to modify CNN's efficiency. Another major issue in deep learner was that data from real-world examples were not necessarily distributed extensively across classes [9].

As a result, when building the CNN for recognizing FDs, two critical objectives were taken into account: the regeneration of constrained patterns and the handling of an unbalanced sample. To eliminate discrepancies on fabric visuals, the fundamental CNN must not have several convolutional layers and ought to keep visual continuity in feature maps by pooling. In this context, the PPAL-CNN model [10] was created to identify FDs using probabilistic error characteristics. To begin, the filament types have been identified using auto-correlation of fabric visuals to assess the repetitive fabric motifs.The motif map was then created by regularizing the cross-correlation. The neuron densities might determine the stability of the fabric forms for creating the probabilistic rule. This rule was employed in CNN as PPAL to connect neurons in a motif vicinity to the faulty decision. Further, the flaw risk map has been employed as the adaptive activation map of a CNN, alongside Conditional Random Field (CRF)'s pairwise-potential factor, to properly recognize constrained motifs and handle dysfunctional visuals in CNN training. However, instead of being learned, the CRF must be given a prior distribution. It was difficult to build sophisticated relationships across FD tags if there were many or long-deep relationships.

To address this issue, an EPPAL-CNN model [11] that handles the difficult motif relationship of FDs was thus devised. Initially, the CRF has been enhanced by the use of external memory rules suggested by memory channels, allowing CRFs to comprehend localized features and analyze the full image. It has a memory layer as well as a Dynamic CRF (DCRF) layer. The memory layer is divided into three sections: inbound, outbound, and actual inbound memory. The arriving and exiting memories have been specified by an attentiveness algorithm which provides weights depending on the relevance of the

arriving and existing arriving memories. Following that, the memory layer's output has been passed into the DCRF as input.

The multivariate design of the DCRF includes linkages between cotemporal labels as well as the exact creation of restricted risk associations between different labels. As a result, an external memory has been used to build a higher-order Markov association across classes. In contrast, gradient-based optimization techniques for learning CNN's weights exhibit

distinctive convergence behavior, leading to ineffective recognition. So, an EPPAL-OCNN model was suggested [12], which includes an individual weight optimization scheme based on NWM-Adam for resolving CNN's undesirable convergence. A unique first-order gradient descent optimization method is provided in this approach, which employs a dynamic exponential decay rate for second-moment approximation rather than a preset and fixed one. It can also easily change the weighting of prior gradients in the estimation. This innovative exponential smoothing average version was created motivated by the fact that prior gradients were assigned additional memory than existing gradients. Though it increases the rate of identification, it takes more time to create the detective model for each defect.

Also, learning the OCNN structure needs a vast amount of labeled samples and the acquisition of labeled samples was time-consuming.Therefore in this paper, an EPPAL-OMCCNNmodel is proposed to minimize the time required to create more labeled samples for FDD. In this new model, multi-objective active deep learning is applied which minimizes the cost of manual labeling to a specified range. First, the OCNN structure is built depending on some randomly decided samples. Then, more influential samples are suggested for user's labeling and updated to the learning set to modify the OCNN structure. In all epochs, the reliability of unlabeled samples is determined under 2 distinct criteria: labeled samples and the present structure. For the initial objective, the density and relevance are utilized to determine the reliability of unlabeled samples which prevents the data redundancies. For the second objective, the reliability of unlabeled samples is determined based on the uncertainty and tag-based factor which accelerates the convergence of the OCNN and decreases the efficiency variance across labels, correspondingly. Thus, this model can label the more influential samples automatically with the minimum time for recognizing and categorizing the FDs.

The remainder of this paper will be structured as follows: Section II covers prior work on FD recognition. Section III describes the EPPAL-OMCCNN model, while Section IV portrays its effectiveness. Section V ends with a summary and offers potential refinements.

II. LITERATURE SURVEY

Zhang et al. [13] developed a new FD identification scheme depending on the saliency metric for color dissimilarity and positional aggregation. In this scheme, the RGB color space of a

fabric photo was transformed into the color space for defining the features. After that, the color dissimilarity and the positional distance between identical patches were utilized to estimate the faulty ranges. Also, a multi-scale analysis method was executed on the pyramid images of the input fabric image to enhance the contrast between the faulty and non-faulty areas. But, it was still difficult to identify the faults in the motif and box-patterned fabric images.

Wei et al. [14] designed a novel scheme by integrating Compressive Sensing and CNN (CS-CNN) to categorize the FDs. First, the CS was used to compress and augment the data in small sample dimensions. After, the CNN was utilized to categorize the image attributes directly from the CS. But, its efficiency was not poor while reducing the sampling rate.

Saleh et al. [15] developed a fully automated FD identification using additive wavelet transform to improve the energy of the faulty area and attenuate the energy of the

background in the decided range. The trous wavelet was used to extract the approximate sub-image at a suitable range. Also, an improved thresholding scheme depending on statistical determination was applied. However, its accuracy was not effective.

Jing et al. [16] developed a Mobile-Unet to partition the FDs by using the median frequency balancing error factor which solves the data imbalance issue. Also, a depth-wise separable convolution was applied to minimize the complexity and network structure dimension. First, the MobileNetV2 was utilized as the encoder and 5 deconvolution layers were included as the decoder. Then, the softmax unit was employed to create the final partition mask. But, it needs more manually annotated samples for learning because it was a supervised technique.

Di et al. [17] designed an FD identification technique depending on the mixture of lighting correction and visual salient features. First, a multi-scale window box filter was created to mine the lighting element of the image. The created 2D gamma correction factor was utilized to execute the lighting correction on the image at the global angle and the local contrast of the image was enhanced at the local angle. Also, the L0-gradient reduction was used to discard the background texture of fabric images. Then, 2D fractional Fourier transform was applied to acquire the saliency map of the quaternion image. But, it has a high False Positive Rate (FPR) for dot-patterned FDs.

Liu et al. [18] developed an effective weakly supervised shallow network called DLSE-Net with Link-SE (L-SE) unit and Dilation Up-Weight CAM (DUW-CAM) for identifying FDs. Initially, the network has a residual link that was built as a new branch to remove the semantic gap created by the link of various layers. Then, the L-SE unit was used to guide the weights to be concerned with the entire network in global optimization. Moreover, a new DUW-CAM with an attention strategy was applied to enhance the adaptability of the network by suppressing the background and enhancing the fault areas. But, it cannot identify the small defects accurately.

Shi et al. [19] designed an FD identification technique depending on the low-rank decomposition of gradient data and structured graph scheme. The structured graphics scheme was used to split the FD image into a defect-free block with local features and defect damage moments. In the merging task, an adaptive threshold was assigned based on the number of cycles contained in the present block to support intra lattice merging and avoid the merging of defective blocks and neighboring non-defective blocks. Also, the defect prior data computed from the partition outcomes was applied to direct matrix decomposition to weaken the defect-free area and enhance the defect region under the sparse term. On the other hand, it has a high difficulty to attain sparse outcomes and so its robustness was not effective.

III. PROPOSED METHODOLOGY

In this section, the EPPAL-OMCCNN model is explained in brief. Initially, the training fabric samples are represented as $\mathcal{D} = \{x_i, y_i\}_{i=1}^{N}$ where $x_i$is i^{th}input sample in $\mathcal{D}$ and has a string: $\{x_{i1}, \dots, x_{iT}\}$ and y_i is their related labels $\{y_{i1}, \dots, y_{iT}\}$. During EPPAL-OMCCNN learning, all $x_t$define the temporal characteristics in any input sample with their related tag y_t. Figure 1 displays the overall schematic representation of EPPAL-OMCCNN-based FD identification model.

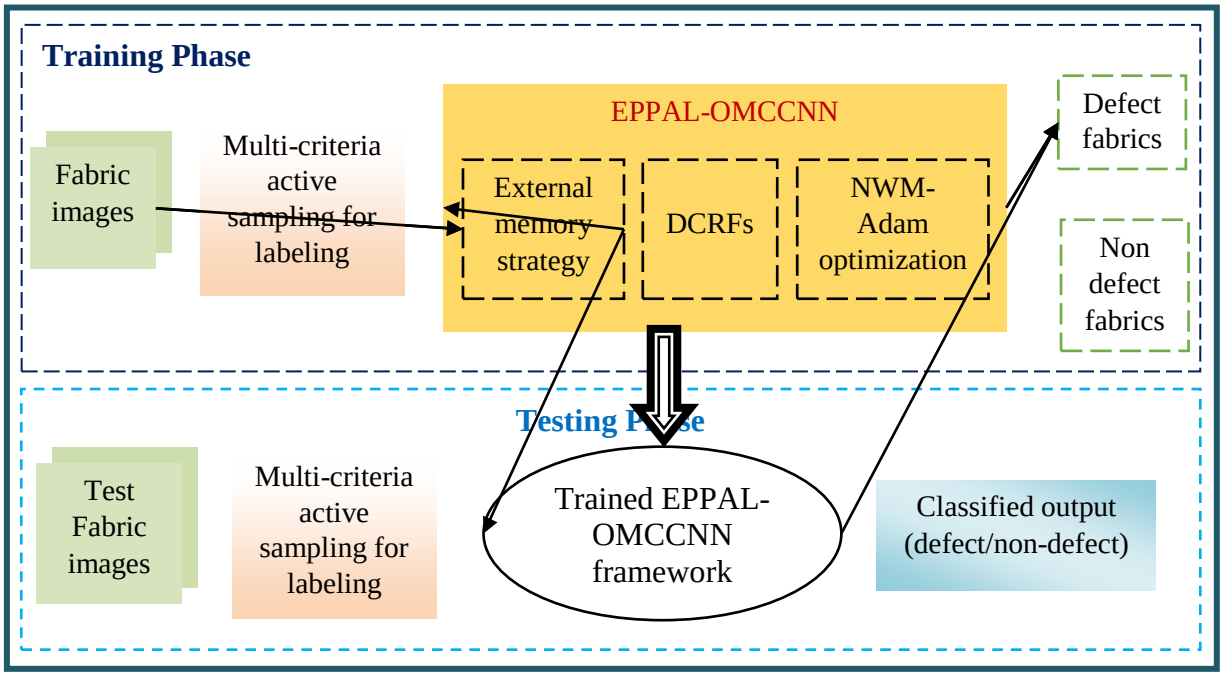

Figure 1. Block Diagram of Proposed FDs Recognition System

Figure 2 depicts the schematic representation of the multi-objective active learning strategy. Primarily, the training fabric samples of both defective and non-defective are gathered at random manner. Then, the PPAL-CNN classifier is built using some randomly selected samples. So, additional influential samples are needed for labeling and then included to the learning set to modify this classifier. In every step, the importance of the unlabeled samples is measured under 2 situations: i) the labeled samples and ii) the current framework.

For the primary situation, density and similarity are utilized to measure the importance of unlabeled samples for minimizing the data redundancy. For the secondary situation, the importance of unlabeled samples is determined in accordance with the uncertainty and label-based measure.So, 2 different types of samples are created to balance among labels and utilized to train the EPPAL-OCNN classifier to recognize FDs.

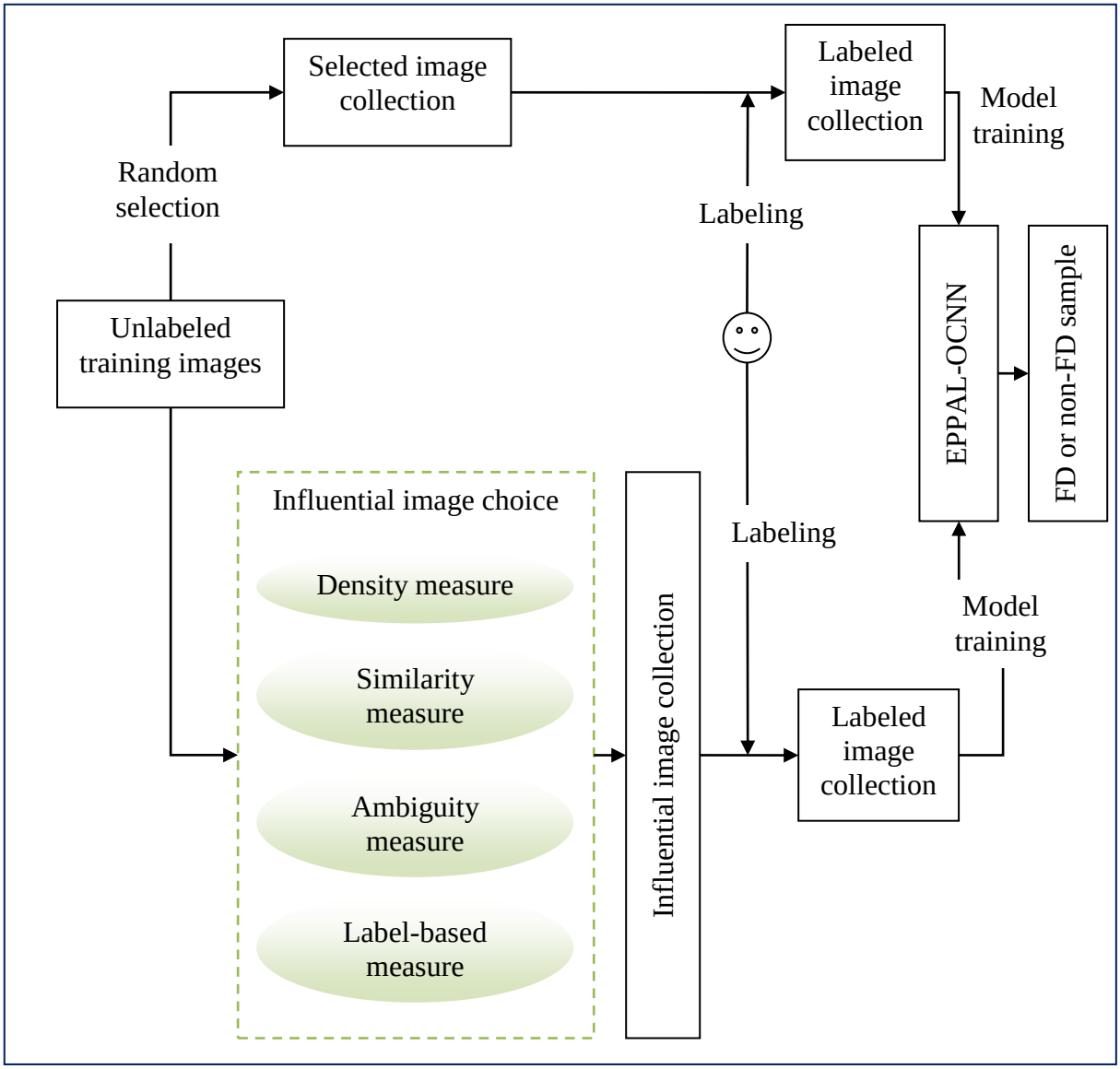

Figure 2. Schematic Representation of Multi-Objective Active Learning Scheme

3.1 Choice of Influential Samples

For an EPPAL-OCNN structure $(\mathcal{S})$ and the labeled image collection $\mathcal{D}_L$, the choice of influential image is intended at providing an influential image collection $\mathcal{D}_I$ from the unlabeled image collection $\mathcal{D}_{UL}$.

The importance of $\mathcal{D}_I$ under the situations $\mathcal{D}_L$ and $\mathcal{S}$ is defined as $imp(\mathcal{D}_I|\mathcal{D}_L,\mathcal{S})$. The influential image choice method is intended at recognizing the image collection $\mathcal{D}_I$ from $\mathcal{D}_{UL}$ to increase the rate of $imp(\mathcal{D}_I|\mathcal{D}_L,\mathcal{S})$ as:

$$\underset{\mathcal{D}_I}{\operatorname{argmax}}\, imp(\mathcal{D}_I|\mathcal{D}_L,\mathcal{S}) \quad (1)$$

Consider that $\mathcal{D}_L$ and $\mathcal{S}$ separately influence the importance of $\mathcal{D}_I$ and Eq. (1) is converted as:

$$\underset{\mathcal{D}_I}{\operatorname{argmax}}\, \alpha imp(\mathcal{D}_I|\mathcal{D}_L) + (1-\alpha) imp(\mathcal{D}_I|\mathcal{S}) \quad (2)$$

In Eq. (2), α denotes the weight to balance the efficiencies of $imp(\mathcal{D}_I|\mathcal{D}_L)$ and $imp(\mathcal{D}_I|\mathcal{S})$. The initial term $imp(\mathcal{D}_I|\mathcal{D}_L)$ is the importance of $\mathcal{D}_I$ under $\mathcal{D}_L$ and the second term $imp(\mathcal{D}_I|\mathcal{S})$ is the importance of $\mathcal{D}_I$ under $\mathcal{S}$.

A. Estimation of Importance under Labeled Images

For $\mathcal{D}_L$, the importance of all images x_i in $\mathcal{D}_I$ is determined according to the density and similarity. Density is the closeness of images. The greater density denotes the irrelevant feature of images and

the marginal importance and vice versa. The importance is determined according to the density is as:

$$imp_{den}(x_i|\mathcal{D}_L) = 1 - \frac{1}{|\mathcal{D}_L^c|}\sum_{x_j \in \mathcal{D}_L^c} Cosd(x_i, x_j) \quad (3)$$

In Eq. (3), p refers to the pseudo-label of x_i by the EPPAL-OCNN framework, $\mathcal{D}_L^p$ refers to the image collection from the label p in $\mathcal{D}_L$ and $Cosd(.,.)$ denotes the cosine distance factor. The density importance is determined by using only the labeled images with a similar label as x_i. Also, the similarity is utilized to guarantee the variety of images. This means that x_i must be varied from another image in $\mathcal{D}_L$. So, the importance is determined according to the similarity is as:

$$imp_{sim}(x_i|\mathcal{D}_L) = 1 - \max_{x_j \in \mathcal{D}_L^c} Cosd(x_i, x_j) \quad (4)$$

Further, such 2 measures are merged with equivalent weights to determine $imp(x_i|\mathcal{D}_L)$as:

$$imp(x_i|\mathcal{D}_L) = \frac{1}{2} imp_{den}(x_i|\mathcal{D}_L) + \frac{1}{2} imp_{sim}(x_i|\mathcal{D}_L) \quad (5)$$

The importance of each image in $\mathcal{D}_I$ is summed as$imp(\mathcal{D}_I|\mathcal{D}_L)$ and the greater value of $imp(\mathcal{D}_I|\mathcal{D}_L)$ guarantees that the images in $\mathcal{D}_I$ have rich and non-recurring features.

B. Estimation of Importance under EPPAL-OCNN Model

For $\mathcal{S}$, the importance of $\mathcal{D}_I$ is associated with 2 different parameters. The primary parameter is the ambiguity measure. The indistinguishable images give indistinct features to speed up the convergence of the EPPAL-OCNN framework. The second parameter is the label-based measure applied for choosing highly valuable labels and avoiding efficiency discrepancy among labels. Such 2 parameters are merged as:

$$imp(x_i|\mathcal{S}) = \beta imp_{amb}(x_i|\mathcal{S}) + (1-\beta) imp_{lab}(x_i|\mathcal{S}) \quad (6)$$

In Eq. (6), β refers to the weight to stabilize these 2 parameters. The importance of every image in $\mathcal{D}_I$ is summed as:

$$imp(\mathcal{D}_I|\mathcal{S}) = \sum_{i=1}^{N} imp(x_i|\mathcal{S}) \quad (7)$$

To determine the ambiguity, a modified margin sampling scheme is adopted. Consider $P(C_m|x_i, \mathcal{S})$ is the posterior possibility of the unlabeled image x_i belonging to the class C_m under $\mathcal{S}$ and$imp_{amb}(x_i|\mathcal{S})$ is determined as:

$$Mean_K(x_i|\mathcal{S}) = \frac{1}{K}\sum_{m=1}^{K} P(C_m|x_i, \mathcal{S}) \quad (8)$$

$$imp_{amb}(x_i|\mathcal{S}) = 1 - \frac{1}{K}\sum_{m=1}^{K} |P(C_m|x_i, \mathcal{S}) - Mean_K(x_i|\mathcal{S})| \quad (9)$$

In Eqns. (8) & (9), C_m denotes the label of m^{th} possible class, K refers to the top K possible classes and $Mean_K(x_i|\mathcal{S})$ defines the average value of the top K chances. The range of K is determined while the total of the top K chances is slightly over $\frac{1}{2}$ in the testing. Also, the label-based measure is used to decide 2 categories of images. The initial category is the images from the classes that reveal quick efficiency enhancement. Such images reveal the possibility to speed up the efficiency enhancement of the EPPAL-OCNN structure.

The second category is the images from the classes that show poor efficiency. Such images are employed to get an efficiency tradeoff among classes. Consider Acc_t^c is the classification accurate of c^{th} class by $\mathcal{S}$ in epoch t on the test images. After that, a weight is assigned to c^{th} class as:

$$W_t^c = \begin{cases} max\left(0, \frac{(Acc_t^c - Acc_{t-1}^c)}{Z_1}\right), & \min Acc_t^c < th \\ \frac{1/Acc_t^c}{Z_2}, & \min Acc_t^c \geq th \end{cases} \quad (10)$$

In Eq. (10), Z_1 and Z_2 are regularization variables and th is a threshold. This model focuses on the images from the classes that enclosethe best efficiency improvement. The efficiency improvement of all classes is analyzed by the efficiency variance between t^{th} and $(t-1)^{th}$epochs on the testing images. Since the efficiency prolongs to enhance, this model provides images from the classes with poor efficiency to tradeoff the efficiency amid classes.

For an unlabeled image x_i in t, its most analogous image x_a is determined on visual space in $\mathcal{D}_L$ and then the label a of x_a is set to x_i as its pseudo-label. Moreover, the value of $imp_{lab}(x_i|\mathcal{S})$ is equivalent to W_t^a.

C. Parameter fine-tuning

In this model, the value of α and β in Eqns. (2) & (6) are adaptively fine-tuned. At the starting of learning, the EPPAL-OCNN framework shows a poor efficiency and its estimated chance is not reliable. So, the metrics are considered depending on the labeled images such as similarity and density. As a result, an incredibly high range is assigned for α in the primary step. Since the learning continues, the efficiency of the EPPAL-OCNN keeps on enhancing and the chance estimated by the EPPAL-OCNN turns into realistic. Similarly, the impact of similarity and density initiates to moderate. So, the range of α is decreased regularly as:

$$\alpha = \alpha_{pri} e^{-Acc_t} \quad (11)$$

In Eq. (11), α_{pri} denotes the primary value and Acc_t refers to the mean classification accuracy with the test set in t^{th} epoch. Similarly, the variable β is utilized to normalize the level of importance between the ambiguity and the label-based measure. In the early epochs of learning, assume that $\mathcal{S}$ does not able to perfectly predict labels; thus, the label-based measure is termed unreliable. Accordingly, this presented model highly concentrates on the ambiguity via allocating the great range to β to speed up the convergence. Since the accuracy enhances and the convergence rate reduces, the credibility of the label is analyzed. So, the range of β is decreased slowly as:

$$\beta = \beta_{pri} e^{-Acc_t} \quad (12)$$

In Eq. (11), β_{pri} denotes the primary value. Thus, the efficiency of FD recognition is enhanced successfully by alleviating the class imbalance challenge.

Algorithm:

Input: Training dataset $\mathcal{D} = \{x_i, y_i\}_{i=1}^N$

Output: Defective fiber samples and non-defective fiber samples

Begin

Initialize the labeled image collection $\mathcal{D}_L^t$, unlabeled image collection $\mathcal{D}_{UL}^t$, primary collection dimension N_{pri}, the maximum epoch T, the number of chosen images in all epochs N and the primary range of variables $\alpha_{pri}, \beta_{pri}$;

$\mathcal{D}_{UL}^0 = \mathcal{D}, \mathcal{D}_L^0 = \{\}$;

Choose N_{pri} images from $\mathcal{D}_{UL}^0$ at random manner and include them to $\mathcal{D}_I$;

$\mathcal{D}_{UL}^1 = \mathcal{D}_{UL}^0 - \mathcal{D}_I, \mathcal{D}_L^1 = \mathcal{D}_L^0 + \mathcal{D}_I, \mathcal{D}_I = \{\}$;

Learn the EPPAL-OCNN $\mathcal{S}^1$ by utilizing $\mathcal{D}_L^1$;

Determine α and β using Eqns. (11) & (12);

$\boldsymbol{for}(t = 1:T)$

  $\boldsymbol{for}(every\ image\ x_i\ in\ \mathcal{D}_{UL}^t)$

    Compute $imp(x_i|\mathcal{D}_L^t)$ using Eq. (5) and$imp_{amb}(x_i|\mathcal{S}^t)$ using Eq. (9);

    Compute $imp_{lab}(x_i|\mathcal{S}^t) = W_t^a$;

    Compute $imp(x_i|\mathcal{S}^t)$ using Eq. (6) and the importance value for x_i as:

      $$imp(x_i|\mathcal{S}^t, \mathcal{D}_L^t) = \alpha imp(x_i|\mathcal{D}_L) + (1-\alpha) imp(x_i|\mathcal{S})$$

  $\boldsymbol{end\ for}$

  Include the top N unlabeled images $\{x_i\}_{i=1}^N$with the highest importance to $\mathcal{D}_I$;

  $\mathcal{D}_{UL}^{t+1} = \mathcal{D}_{UL}^t - \mathcal{D}_I, \mathcal{D}_L^{t+1} = \mathcal{D}_L^t + \mathcal{D}_I, \mathcal{D}_I = \{\}$;

  Learning the classifier $\mathcal{S}^{t+1}$ depending on $\mathcal{D}_L^{t+1}$;

  Fine-tune the variables α and β using Eqns. (11) & (12);

$\boldsymbol{end\ for}$

Apply the test image samples to recognize the defective and non-defective image samples;

Validate the classifier performance;

End

IV. EXPERIMENTAL RESULTS

In this part, the efficiency of EPPAL-OMCCNN is analyzed by implementing it in MATLAB 2017b and compared with the existing models. The considered existing models are EPPAL-OCNN [12], EPPAL-CNN [11], CS-CNN [14] and Mobile-Unet [16]. In this analysis, The Irish Longitudinal Study on Ageing (TILDA) image corpus [20] is considered which includes 7 labels of fibers with flaws and 1 label of fibers without flaws. As a consequence, a complete corpus contains 3200 TIF visuals totaling 1.2GB in size. Each image in the TILDA collection contains a full description of the image's flaws. Amongst, 2100 images are used for learning and 1100 visuals are used for testing. The analysis is focused on different metrics associated with the identification.Table 1 presents the confusion matrix for all classes is obtainedindependently and a mean of recognized results for EPPAL-OMCCNN.

Table 1.Confusion Matrix for EPPAL-OMCCNN using 1100 Test Images

	Recognized Class		
Actual Class		Positive	Negative
	Positive (550 for each class)	True Positive **530**	False Negative **20**
	Negative(550 for other class)	False Positive **21**	True Negative **529**

4.1 Accuracy

It is the proportion of properly recognized defective and non-defective fiber samples.

$$Acc = \frac{True\ Positive\ (TP)+True\ Negative(TN)}{TP+TN+False\ Positive\ (FP)+False\ Negative(FN)} \times 100\%$$

TP defines the quantity of defective fiber samples properly recognized as defective, TN defines the quantity of non-defective fiber samples perfectly recognized as non-defective. Also, FP defines the quantity of defective fiber samples improperly recognized as non-defective and FN defines the quantity of non-defective fiber samples improperly recognized as defective.

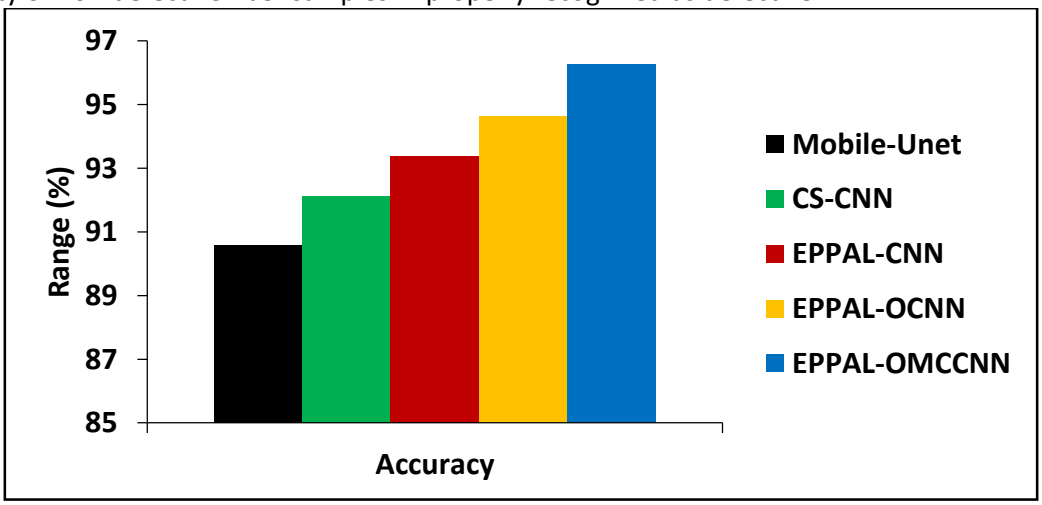

Figure 2. Comparison of Accuracy

Figure 2 demonstrates the accuracy (in %) achieved by the EPPAL-OMCCNN, EPPAL-OCNN, EPPAL-CNN,CS-CNN and Mobile-Unet models. It analyzes that the accuracy of EPPAL-OMCCNN is 6.28% higher than the Mobile-Unet, 4.48% higher than the CS-CNN, 3.12% higher than the EPPAL-CNN and 1.72% higher than the EPPAL-OCNN models because of alleviating the class imbalance problem during learning. Thus, this EPPAL-OMCCNN can maximize the accuracy of recognizing the FDs compared to the other models.

4.2 Precision

It is the proportion of recognized actual defective fiber samples.

eISSN1303-5150

$$Pre = \frac{No.of\ properly\ recognized\ defective\ fibers}{No.of\ properly\ recognized\ defective\ fibers + No.of\ improperly\ recognized\ defective\ fibers}$$

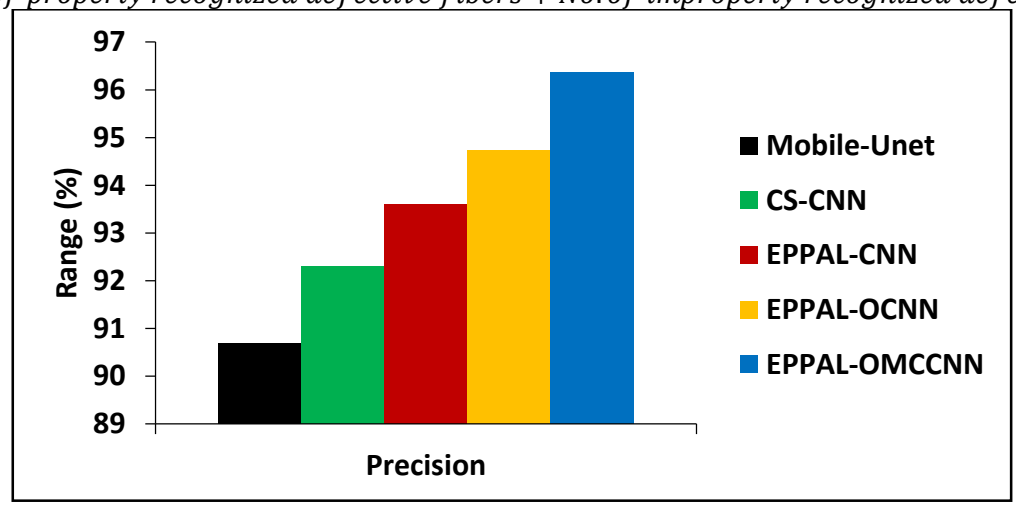

Figure 3. Comparison of Precision

Figure 3portrays the precision (in %) obtained by the EPPAL-OMCCNN, EPPAL-OCNN, EPPAL-CNN, CS-CNN and Mobile-Unet models. It indicates that the precision of EPPAL-OMCCNN is 6.25% greater than the Mobile-Unet, 4.39% greater than the CS-CNN, 2.95% greater than the EPPAL-CNN and 1.72% greater than the EPPAL-OCNN models. So, this EPPAL-OMCCNN increases the precision of identifying the FD by solving the class imbalance problem.

4.3 Recall

It is the proportion of defective fiber visuals properly recognized as faulty.

$$Rc = \frac{No.of\ properly\ recognized\ defective\ fibers}{No.of\ properly\ recognized\ defective\ fibers + No.of\ improperly\ recognized\ non-defective\ fibers}$$

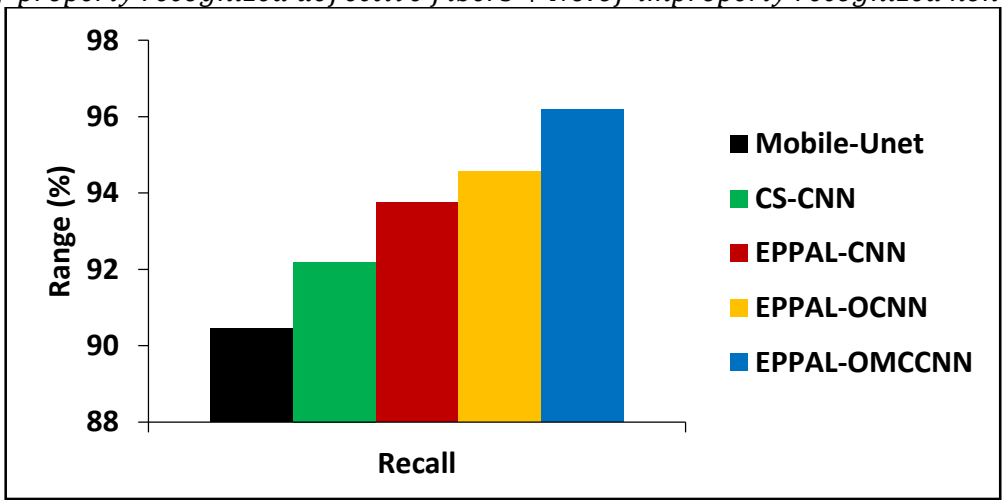

Figure 4. Comparison of Recall

Figure 4 displays the recall (in %) obtained by the EPPAL-OMCCNN, EPPAL-OCNN, EPPAL-CNN, CS-CNN and Mobile-Unet models. It indicates that the recall of EPPAL-OMCCNN is 6.3% greater than the Mobile-Unet, 4.3% greater than the CS-CNN, 2.6% greater than the EPPAL-CNN and 1.7% greater than the EPPAL-OCNN models. So, this EPPAL-OMCCNN increases the recall of identifying the FD by integrating the multi-objective active learning to alleviate the class imbalance problem.

4.4 F-measure

It is the harmonic average of Pr and Rc.

$$F - measure = 2 \times \frac{Pr \cdot Rc}{Pr + Rc}$$

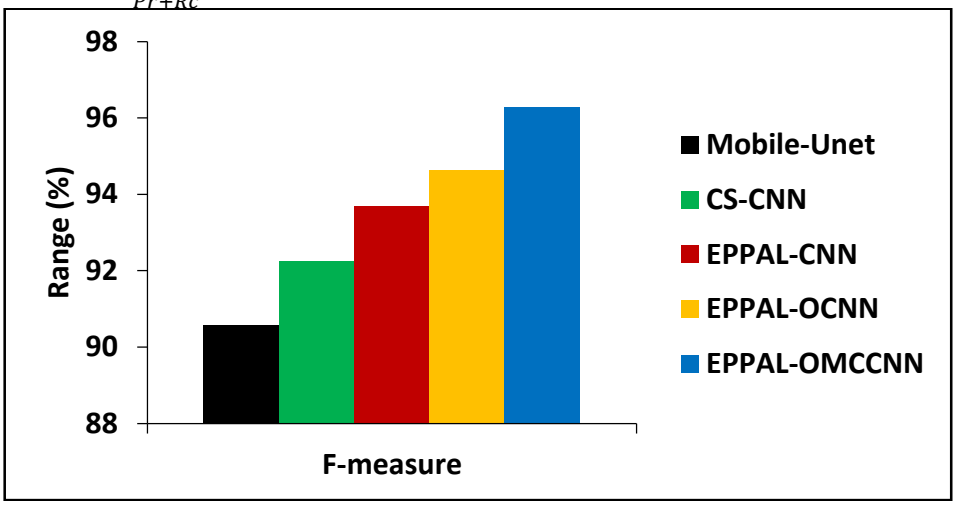

Figure 5. Comparison of F-measure

Figure 5 illustrates the f-measure (in %) obtained by the EPPAL-OMCCNN, EPPAL-OCNN, EPPAL-CNN, CS-CNN and Mobile-Unet models. It addresses that the f-measure of EPPAL-OMCCNN is 6.3% greater than the Mobile-Unet, 4.4% greater than the CS-CNN, 2.8% greater than the EPPAL-CNN and 1.7% greater than the EPPAL-OCNN models. So, this EPPAL-OMCCNN increases the f-measure compared to all other models to recognize the FD effectively by balancing the efficiency among classes.

V. CONCLUSION

This study presented an EPPAL-OMCCNN model which employs the multi-objective active learning to reduce the labeling cost and solve the class imbalance problem during training. At first, the EPPAL-OCNN architecture was built with the help of limited training images. Then, the multi-objective active learning was performed to label more influential images and alter the EPPAL-OCNN classifier for FD recognition. At last, the testing outcomes using TILDA database proved that the EPPAL-OMCCNN has realized 96.27% accuracy which was 3.87% larger than all other models compared to the classical models.However, it should adapt to predict historical and new classes of defect patterns. So, the future work will focus on using reinforcement learning to train and predict any classes of FD patterns effects.

REFERENCES

[1] Ahmed, M., Islam, T., & Ali, M. D. S. (2019). Study on different types of defects and their causes and remedies in garments industry. *Journal of Textile Engineering & Fashion Technology*, *5*(6), 300-304.

[2] Yapi, D., Mejri, M., Allili, M. S., & Baaziz, N. (2015). A learning-based approach for automatic defect detection in textile images. *IFAC-PapersOnLine*, *48*(3), 2423-2428.

[3] Rasheed, A., Zafar, B., Rasheed, A., Ali, N., Sajid, M., Dar, S. H., ... & Mahmood, M. T. (2020). Fabric defect detection using computer vision techniques: a comprehensive review. *Mathematical Problems in Engineering*, *2020*, 1-24.

[4] Li, C., Li, J., Li, Y., He, L., Fu, X., & Chen, J. (2021). Fabric defect detection in textile manufacturing: a survey of the state of the art. *Security and Communication Networks*, *2021*, 1-13.

[5] Dong, X., Taylor, C. J., & Cootes, T. F. (2018). Small defect detection using convolutional neural network features and random forests. In *Proceedings of the European Conference on Computer Vision Workshops*, pp. 1-15.

[6] Henn, M. A., Zhou, H., & Barnes, B. M. (2019). Data-driven approaches to

optical patterned defect detection. *OSA continuum*, *2*(9), 2683-2693.

[7] Jun, X., Wang, J., Zhou, J., Meng, S., Pan, R., & Gao, W. (2021). Fabric defect detection based on a deep convolutional neural network using a two-stage strategy. *Textile Research Journal*, *91*(1-2), 130-142.

[8] Iqbal Hussain, M. A., Khan, B., Wang, Z., & Ding, S. (2020). Woven fabric pattern recognition and classification based on deep convolutional neural networks. *Electronics*, *9*(6), 1-12.

[9] Hu, Y., Long, Z., Sundaresan, A., Alfarraj, M., AlRegib, G., Park, S., & Jayaraman, S. (2021). Fabric surface characterization: assessment of deep learning-based texture representations using a challenging dataset. *The Journal of the Textile Institute*, *112*(2), 293-305.

[10] Ouyang, W., Xu, B., Hou, J., & Yuan, X. (2019). Fabric defect detection using activation layer embedded convolutional neural network. *IEEE Access*, *7*, 70130-70140.

[11] Vinothini, B., & Sheeja, S. (2021).Memory enhanced dynamic conditional random fields embedded pairwise potential CNN for fabric defects identification. *International Journal of Engineering Trends and Technology*, *69*, 227-234.

[12] Zhang, K., Yan, Y., Li, P., Jing, J., Liu, X., & Wang, Z. (2018). Fabric defect detection using salience metric for color dissimilarity and positional aggregation. *IEEE Access*, *6*, 49170-49181.

[13] Wei, B., Hao, K., Tang, X. S., & Ding, Y. (2019). A new method using the convolutional neural network with compressive sensing for fabric defect classification based on small sample sizes. *Textile Research Journal*, *89*(17), 3539-3555.

[14] Saleh, E. H., Fouad, M. M., Sayed, M. S., Badawy, W., El-Samie, A., & Fathi, E. (2020). Fully automated fabric defect detection using additive wavelet transform. *Menoufia Journal of Electronic Engineering Research*, *29*(2), 119-125.

[15] Jing, J., Wang, Z., Rätsch, M., & Zhang, H. (2020). Mobile-Unet: An efficient convolutional neural network for fabric defect detection. *Textile Research Journal*, 1-13.

[16] Di, L., Long, H., & Liang, J. (2020). Fabric defect detection based on illumination correction and visual salient features. *Sensors*, *20*(18), 5147.

[17] Liu, Z., Huo, Z., Li, C., Dong, Y., & Li, B. (2021). DLSE-Net: a robust weakly supervised network for fabric defect detection. *Displays*, *68*, 1-10.

[18] Shi, B., Liang, J., Di, L., Chen, C., & Hou, Z. (2021). Fabric defect detection via low-rank decomposition with gradient information and structured graph algorithm. *Information Sciences*, *546*, 608-626.

[19] https://lmb.informatik.uni-freiburg.de/resources/datasets/tilda.en.html